One-pot synthesis and characterizations of bi-functional phosphor–magnetic @SiO_2 nanoparticles: controlled and structured association of Mo_6 cluster units and γ-Fe_2O_3 nanocrystals†

Fabien Grasset,*[a] Frédérick Dorson,[a] Yann Molard,[a] Stéphane Cordier,*[a]
Valérie Demange,[ab] Christiane Perrin,[a] Valérie Marchi-Artzner[a] and
Hajime Haneda*[c]

Received (in Cambridge, UK) 23rd April 2008, Accepted 18th July 2008
First published as an Advance Article on the web 5th September 2008
DOI: 10.1039/b806919k

Nanostructured silica coated bifunctional nanoparticles based on $[Mo_6Br_{14}]^{2-}$ units as phosphorescent dye and magnetic γ-Fe_2O_3 nanocrystals were synthesized and characterized.

Research on luminescent inorganic nanomaterials is gaining in interest since they could find applications as luminescent dyes in biolabelling nanotechnologies because they appear more photostable than their organic homologous. For imaging applications, the widely studied inorganic quantum dots (QD) encounter several challenges, such as a potential toxicity[1] and a limited tissue penetration for visible emission.[2] To address these needs, it is important to develop lower toxicity near-infrared-emitters in order to improve tissue penetration depth.[1,3] Recently, we reported a low temperature water-in-oil (W/O) microemulsion preparation of near-infrared phosphor nanoparticles, $Cs_2Mo_6Br_{14}$@SiO_2, built up from discrete nanosized $[Mo_6L_{14}]^{2-}$ inorganic cluster units (L = Cl, Br, I) dispersed in a silica matrix.[4] Regarding the optical properties of tissue, it turns out that these nanoparticles are relevant candidates in bioimaging strategies and labelling. Indeed, the haemoglobin absorption spectrum significantly decreases above 600 nm, and the absorption due to water content begins to rise at 900 nm. Moreover, the surface of the SiO_2 matrix can easily be conjugated with various biomolecules and is water-soluble and biocompatible.[5] On the other hand, owing to finite-size effects,[6] the magnetic properties of inorganic nanoparticles (*e.g.* magnetite Fe_3O_4, maghemite γ-Fe_2O_3) are of great interest in a wide range of applications, including magnetic fluids, catalysis, magnetic resonance imaging, biotechnology/biomedicine. . .[7] For instance, the simple synthesis of functionalized Fe_3O_4 superparamagnetic/silica core/shell nanoparticles and their application as magnetically separable high performance biocatalysts was recently reported.[8] Contrary to γ-Fe_2O_3, several examples evidence that unfortunate redox effects occur on magnetite Fe_3O_4 nanocrystals.[9] Moreover, γ-Fe_2O_3-based nanoparticles are magnetically handleable, sensitive to radiofrequency signals and non-toxic materials. The control of the γ-Fe_2O_3 nanocrystals size and their magnetic properties are already well-mastered technologies.[7]

The preparation and characterization of bifunctional magnetic/luminescent nanocomposites for biological applications is a field of research that is actually in a stage of rapid development. Several strategies of synthesis are reported: (i) direct grafting of organic dyes onto magnetic nanoparticles *via* a reactive aminosilane molecule,[10] (ii) core/shell strategy,[11] (iii) simultaneous encapsulation of hydrophobic CdSe/ZnS QDs and magnetic γ-Fe_2O_3 nanoparticles into water-soluble micelles.[12] In this context, the combination of luminescent properties of $[Mo_6Br_{14}]^{2-}$ cluster units along with magnetic properties of γ-Fe_2O_3 nanocrystals into @SiO_2 nanoparticles is a technical challenge that will greatly enlarge the range of applications of Mo_6 clusters-based nanoparticles from biolabelling to bioseparation or targeting imaging using MRI techniques.

In this work, a very simple one-pot procedure for the preparation of bifunctional magnetic/luminescent nanoparticles, namely γ-Fe_2O_3–$Cs_2Mo_6Br_{14}$@SiO_2 (**1**), is reported. Nanoparticles were characterized by BF-TEM (bright-field transmission electron microscopy), EELS (electron energy loss spectroscopy), HAADF-STEM (high angular annular dark field-scanning TEM), photoluminescence, susceptibility measurements and optical microscopy under laser irradiation with and without an applied magnetic field. They exhibit a regular spherical shape of 50 nm in diameter; the γ-Fe_2O_3 nanocrystals are located at the centre of the particles whilst the $[Mo_6Br_{14}]^{2-}$ cluster units are homogeneously dispersed around the magnetic core within the @SiO_2 matrix.

The inorganic $Cs_2Mo_6Br_{14}$ precursor has been synthesized according to the procedure described in ref. 13. Monodispersed sols were obtained by dissolution of $Cs_2Mo_6Br_{14}$ powder into an acidic ethanol aqueous solution (50–50) to yield Cs^+ cations and $[Mo_6Br_{14}]^{2-}$ units in solution (10^{-2} mol L^{-1}; pH = 2). Meanwhile, a colloidal aqueous solution of γ-Fe_2O_3 nanocrystals was prepared according to ref. 14. The bifunctional silica nanoparticles have been prepared by W/O microemulsion techniques[4,15] using *n*-heptane as oil phase and Brig30® as surfactant. The aqueous phase contained the two colloidal solutions, TEOS and NH_3(aq). The micro-emulsion was prepared by adding the freshly prepared γ-Fe_2O_3 colloidal

---

[a] *Université de Rennes 1, UMR « Science Chimiques de Rennes » UR1-CNRS 6226, Campus de Beaulieu, CS 74205, F-35042 Rennes Cedex, France. E-mail: fabien.grasset@univ-rennes1.fr; stephane.cordier@univ-rennes1.fr*
[b] *Nancy-Université, UMR LSGS, INPL-CNRS 7570, Ecole des Mines, CS 14234, F-54042 Nancy Cedex, France*
[c] *National Institute for Materials Science, Namiki 1-1, Tsukuba, Ibaraki, 305-0044, Japan. E-mail: Haneda.hajime@nims.go.jp*

† Electronic supplementary information (ESI) available: Representation of $Mo_6L^i_8L^a_6$ units, luminescence spectra, magnetization curves of **1** (FC, ZFC), electron diffraction patterns. See DOI: 10.1039/b806919k

solution into the surfactant/heptane mixture followed after few minutes by the metal atom clusters colloidal solution. The optical transparency of the resulting solution indicated the formation of W/O microemulsion. After addition of TEOS as silica precursor into the mixture, the silica nanoparticles were grown by increasing the pH inside the droplets with ammonia (NH_3(aq) 28%) that meanwhile catalyzed the condensation of TEOS. After 48 h, the resulting nanoparticles were washed with *n*-heptane, ethanol and acetone (removing oil and surfactants) followed by a separation in a centrifuge at 5000 rpm for 15 min. Energy dispersive spectroscopy analysis performed on a pellet of **1** reveals the presence of all expected elements (Si and O represent roughly 98% of the total composition, Mo/Fe $\approx$ 1/4). The aforementioned synthesis leads to reproducible nanoparticles with a controlled and structured architecture. In first approximation, the control of such architecture and separation design between magnetic core and luminescent clusters could be explained by the difference of polarity between the two initial acidic solutions containing the γ-Fe_2O_3 nanocrystals and the cluster units. Indeed, previous photophysical studies of reverse micelles showed that solutions with low polarity (or high hydrophobicity) reside near the water/oil interface, whereas those with high polarity (or low hydrophobicity) reside at the centre of the reverse micelles.[16] By addition of 50% of ethanol, the polarity of the cluster solution is lower than that of γ-Fe_2O_3, which therefore induces the localization of γ-Fe_2O_3 at the centre of the nanoparticles.

Fig. 1(a) displays a BF image of **1**, which evidenced that silica nanoparticles exhibit a relatively uniform spherical shape with an average diameter of 50 nm. Analysis of EELS spectra demonstrates that iron is exclusively located in the core of the nanoparticles (Fig. 1(b)). Fig. 2 displays HAADF-STEM micrographs of **1**, which confirm the regular spherical shape of nanoparticles. The discrete metal atom clusters, represented by small light spots of *ca.* 1 nm in diameter, are very well dispersed in the @SiO_2 matrix (Fig. 2(b)). This originates from the high quality of the starting sols in which the discrete $[Mo_6X_{14}]^{2-}$ units behave like molecular anions.[4] Electron diffraction investigations prove that the core is crystalline with an indexation in agreement with the γ-Fe_2O_3 structure (ESI†).

An important result is that in this process, the γ-Fe_2O_3 is introduced as the central core of the silica particle, and $Cs_2Mo_6Br_{14}$ as a homogeneous dispersion (*ca.* 10 Å diameter) interleaved between silica shells yielding very reproducible architecture. This disposition is optimum to maximize the photoluminescence emission.

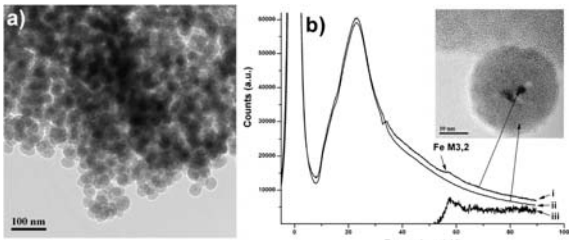

Fig. 1 (a) BF image of **1**. (b) Inset: BF image of a nanoparticle (**1**) and EELS spectra of corresponding nanoparticle core (i) and shell (ii). Nanoparticle core spectrum after background removal (iii).

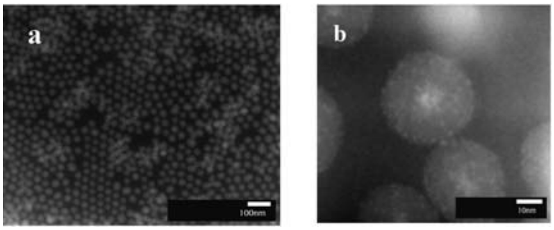

Fig. 2 HAADF-STEM images: (a) light spots at the center of the particles correspond to γ-Fe_2O_3 nanocrystals; (b) view of a nanoparticle evidencing the good dispersion of clusters as small light spots.

$[(Mo_6L^i_8)L^a_6]$ units (a = apical, i = inner) constitute the basic building blocks in the Mo_6 octahedral cluster chemistry.[13] The Mo_6 cluster is face-capped by eight inner ligands (L^i) and is additionally bounded to six apical ligands (L^a) (ESI†). $[Mo_6Br_{14}]^{2-}$ anionic units are highly luminescent nanometric species in the far-red region (Φ = 0.23) with a broad UV-Vis absorption window.[17] This property makes them relevant building blocks for the elaboration of nanomaterials and nanoparticles with luminescent properties interesting for the actual challenges encountered in biotechnologies. In order to evaluate the luminescent properties of $[Mo_6Br_{14}]^{2-}$ embedded in **1**, luminescence spectra were recorded in the solid-state form. They were subsequently compared with those of pure silica nanoparticles synthesized in the same conditions as **1**. The pure silica nanoparticles spectrum (ESI†) shows a broad emission band with a maximum depending on the irradiation wavelength. For instance, irradiation at λ_{exc} = 340 nm induces a high intensity emission centred on 410 nm while irradiation at λ_{exc} = 440 nm in the same conditions reveals a less pronounced emission with a maximum located at 517 nm. Since emission properties of silica particles occur in the broad absorption window of the $[Mo_6Br_{14}]^{2-}$ units, possible interactions between the cluster units and the silica matrix in **1** could be expected. Therefore, the emission spectrum of **1** was recorded using an optimum excitation wavelength of 340 nm to reach, on one hand, a high emission intensity of the @SiO_2 matrix and, on the other hand, the maximum emission intensity of the $[Mo_6Br_{14}]^{2-}$ units (ESI†). Irradiation of **1** at λ_{exc} = 340 nm produced an emission spectrum composed of two bands: a very weak band with a maximum located at λ = 410 nm, corresponding to the emission of the @SiO_2 matrix and an intense band with a maximum located at λ = 738 nm corresponding to the emission of the $[Mo_6Br_{14}]^{2-}$ units. Consequently, it can be concluded that embedding of the cluster results in the almost full quenching of the @SiO_2 matrix emission that may be attributed to an effective energy transfer between the two partners. Moreover, the presence of γ-Fe_2O_3 in the core of the nanoparticles does not affect the luminescence properties of the cluster units that are not oxidized during the process. This important finding is the key point that enables the one-pot synthesis of **1**.

The magnetic behaviour (ESI†) is typical of moderately monodispersed superparamagnetic ferrite nanocrystals dispersed in silica matrix. In ZFC (zero field cooled) mode the magnetization passes through a broad maximum at T_{max} = 30 K characteristic of the freezing of superparamagnetic nanoparticles due to magnetic anisotropy. On cooling the

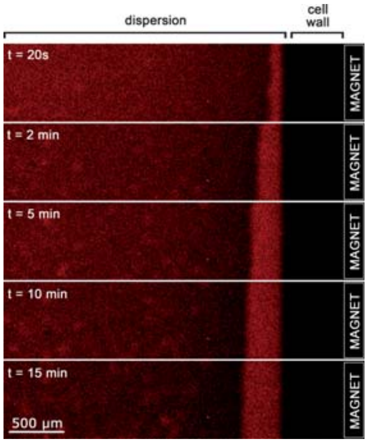

Fig. 3 Optical microscope images using λ_{exc} = 405 nm of dispersed nanoparticles under a magnetic field (1.5 T) showing the growth of a nanoparticles layer along the wall of a cell as a function of time.

FC (field cooled) magnetization coincides with the ZFC magnetization for $T > 70$ K. The non-monodispersity of magnetic nanocrystals is confirmed by the splitting at $T < 70$ K.

The bifunctional character of the nanoparticles has been evidenced by optical microscopy analysis under irradiation at λ_{exc} = 405 nm and applied magnetic field. Fig. 3 shows nicely the effect of an applied magnetic field along the wall of a cell containing dispersed nanoparticles in an aqueous ethanolic solution (pH = 8) as a function of time. For nanobiotechnology application, an important point is that irradiation up to 550 nm (green) is still efficient for the red phosphorescence emission of the $[Mo_6Br_{14}]^{2-}$ cluster core.

Bifunctional silica coated nanoparticles, Fe_3O_4–$Ru(tpy)_3 \cdot Cl_2$@SiO_2, exhibiting similar properties were previously reported.[18] However a multistep procedure was necessary for their synthesis to prevent the luminescence quenching of the $Ru(tpy)_3$ complexes by Fe_3O_4 nanocrystals. In a first step, Fe_3O_4@SiO_2 magnetic cores were prepared and were then coated by $(Ru(bpy)_3)^{2+}$ complexes as luminescent dye. Beyond increased time, the multistep procedures yield rather larger nanoparticles with a diameter of about 100 nm. The main advantage of the process reported here compared to multistep reactions is that the nanoparticles size is divided by a factor 2; this is of very significant interest for their use in biotechnologies.

Recently, monodispersed silica nanoparticles with a 60 nm diameter encapsulating upconversion (UC) green fluorescent emitting nanocrystals ($NaYF_4$:20%Yb,2%Er) and Fe_3O_4 superparamagnetic nanocrystals have been reported with a size of 10 and 16 nm, respectively.[11] They exhibit inverse properties of those reported in this work (*i.e.* red excitation/green emission).

To conclude, the one-pot synthesis reported here leads to reproducible well-structured nanoparticles with a regular spherical shape of about 50 nm in diameter. It is of note that the superparamagnetic γ-Fe_2O_3 nanocrystals are located at the centre of the nanoparticles and $[Mo_6Br_{14}]^{2-}$ phosphorescent units are homogeneously dispersed in the silica coating. The bifunctional character has been evidenced by magnetic susceptibility and luminescence measurements. No quenching interactions were evidenced between γ-Fe_2O_3 nanocrystals and $[Mo_6Br_{14}]^{2-}$ units. Thanks to the easy functionalization of the SiO_2 matrix, the bifunctional γ-Fe_2O_3–$Cs_2Mo_6Br_{14}$@SiO_2 nanoparticles constitute relevant candidates for biotechnologies. Indeed their phosphor properties in the near infrared region (580–900 nm) associated with the magnetism of γ-Fe_2O_3 nanocrystals leads to a large set of potential applications in bioimaging, biolabelling and bioseparation strategies.

This work was supported by the University of Rennes 1, CNRS, NIMS, Fondation Langlois, Region Bretagne and C'Nano Nord-Ouest. The authors thank T. Sasaki for TEM characterization and T. Guizouarn for SQUID measurements.

Notes and references

1 N. Gaponik, I. L. Radtchenko, M. R. Gerstenberger, Y. A. Fedutik, G. B. Sukhorukov and L. Rogach, *Nano Lett.*, 2003, **3**, 369.
2 D. K. Chatterjee, A. J. Rufaihah and Y. Zhang, *Biomaterials*, 2008, **29**, 937.
3 Z. Q. Li and Y. Zhang, *Angew. Chem., Int. Ed.*, 2006, **45**, 7732.
4 F. Grasset, F. Dorson, S. Cordier, Y. Molard, C. Perrin, T. Sasaki, H. Haneda, Y. Bando and M. Mortier, *Adv. Mater.*, 2008, **20**, 143.
5 I. I. Slowing, B. G. Trewyn and Vi S.-Y. Lin, *J. Am. Chem. Soc.*, 2007, **129**, 8845; J. Lu, M. Liong, J. I. Zink and F. Tamanoi, *Small*, 2007, **3**, 1341.
6 H. Lu, E. L. Salabas and F. Schüth, *Angew. Chem., Int. Ed.*, 2007, **46**, 1222.
7 S. Mornet, S. Vasseur, F. Grasset and E. Duguet, *J. Mater. Chem.*, 2004, **14**, 2161; Lu E. L. Salabas and F. Schüth, *Angew. Chem., Int. Ed.*, 2007, **46**, 1222; C. Corot, P. Robert, J. M. Idée and M. Port, *Adv. Drug Delivery Rev.*, 2006, **58**, 1471.
8 J. Lee, Y. Lee, J. K. Youn, H. B. Na, T. Yu, H. Kim, S. M. Lee, Y. M. Koo, J. H. Kwak, H. G. Park, H. N. Chang, M. Hwang, J. G. Park, J. Kim and T. Hyeon, *Small*, 2008, **4**, 143.
9 In *'De la solution à l'oxyde'*, ed. J. P. Jolivet, 1994, InterEditions, CNRS Edition, Paris, ISBN 2729605266.
10 F. Grasset, S. Mornet, A. Demourgues, J. Portier, J. Bonnet, A. Vekris and E. Duguet, *J. Magn. Magn. Mater.*, 2001, **234**, 409.
11 See the references in the review: V. Salgueirino-Maceira and M. A. Correa-Duarte, *Adv. Mater.*, 2007, **19**, 4131; Z. Liu, G. Yi, H. Zhang, J. Ding, Y. Zhang and J. Xue, *Chem. Commun.*, 2008, 694.
12 V. Roullier, F. Boulmedais, F. Grasset, O. Cador and V. Marchi-Artzner, *Chem. Mater.*, in press.
13 K. Kirakci, S. Cordier and C. Perrin, *Z. Anorg. Allg. Chem.*, 2005, **631**, 411; S. Cordier, K. Kirakci, D. Mery, C. Perrin and D. Astruc, *Inorg. Chim. Acta*, 2006, **359**, 1705; D. Mery, L. Plault, C. Ornelas, J. Ruiz, S. Nlate, D. Astruc, J. C. Blais, J. Rodrigues, S. Cordier, K. Kirakci and C. Perrin, *Inorg. Chem.*, 2006, **45**, 1156.
14 R. Massart, *IEEE Trans. Magn.*, 1982, **17**, 1247; S. Mornet, F. Grasset, J. Portier and E. Duguet, *Eur. Cells Mater.*, 2002, **3**, 110. An aqueous colloidal suspension was prepared according to the Massart process: Fe_3O_4 nanocrystals were first obtained by making alkaline an aqueous mixture of $Fe(SO_4)_2$ and $Fe(NO_3)_3$ ([1 mol/L], Fe^{2+}/Fe^{3+} = 0.5) at room temperature. After precipitation, the Fe_3O_4 nanocrystals were chemically oxidized into γ-Fe_2O_3. To obtain a stable aqueous colloidal dispersion of γ-Fe_2O_3 a sufficient electrostaticrepulsion between nanocrystals is needed. The nanocrystals were dispersed in HNO_3 (15 min, 2 mol L^{-1}) under stirring. The acidic precipitate was isolated by decantation on a magnet and/or centrifugation (5000 rpm, 15 min), washed in acetone and dispersed in H_2O. The pH value of the ferrofluid was ≈2.
15 F. Grasset, N. Labhsetwar, D. Li, D. C. Park, N. Saito, H. Haneda, O. Cador, T. Roisnel, S. Mornet, E. Duguet, J. Portier and J. Etourneau, *Langmuir*, 2002, **18**, 8209; F. Grasset, R. Marchand, A. M. Marie, D. Fauchadour and F. Fajardie, *J. Colloid Interface Sci.*, 2006, **299**, 726.
16 S. Chatterjee, R. K. Mitra, B. K. Paul and S. C. Bhattacharya, *J. Colloid Interface Sci.*, 2006, **298**, 935.
17 A. W. Maverick, J. S. Najdzionek, D. MacKenzie, D. G. Nocera and H. B., *J. Am. Chem. Soc.*, 1983, **105**, 1878.
18 L. Zhang, B. Liu and S. Dong, *J. Phys. Chem. B*, 2007, **111**, 10448.